

A novel simple extracellular leucine-rich repeat (eLRR) domain protein from rice (OsLRR1) enters the endosomal pathway and interacts with the hypersensitive-induced reaction protein 1 (OsHIR1)

LIANG ZHOU¹, MING-YAN CHEUNG¹, QI ZHANG², CAI-LIN LEI², SHI-HONG ZHANG^{1,3}, SAMUEL SAI-MING SUN¹ & HON-MING LAM¹

¹Department of Biology and State Key Laboratory of Agrobiotechnology, The Chinese University of Hong Kong, Shatin, Hong Kong, ²Institute of Crop Sciences, The Chinese Academy of Agricultural Sciences, Beijing, China and ³Plant Science College, Jilin University, Changchun, China

ABSTRACT

Receptor-like protein kinases (RLKs) containing an extracellular leucine-rich repeat (eLRR) domain, a transmembrane domain and a cytoplasmic kinase domain play important roles in plant disease resistance. Simple eLRR domain proteins structurally resembling the extracellular portion of the RLKs may also participate in signalling transduction and plant defence response. Yet the molecular mechanisms and subcellular localization in regulating plant disease resistance of these simple eLRR domain proteins are still largely unclear. We provided the first experimental evidence to demonstrate the subcellular localization and trafficking of a novel simple eLRR domain protein (OsLRR1) in the endosomal pathway, using both confocal and electron microscopy. Yeast two-hybrid and *in vitro* pull-down assays show that OsLRR1 interacts with the rice hypersensitive-induced response protein 1 (OsHIR1) which is localized on plasma membrane. The interaction between LRR1 and HIR1 homologs was shown to be highly conserved among different plant species, suggesting a close functional relationship between the two proteins. The function of OsLRR1 in plant defence response was examined by gain-of-function tests using transgenic *Arabidopsis thaliana*. The protective effects of OsLRR1 against bacterial pathogen infection were shown by the alleviating of disease symptoms, lowering of pathogen titres and higher expression of defence marker genes.

Key-words: endosome; HIR1; plant defence response.

INTRODUCTION

Plant receptor-like protein kinases (RLKs) with an extracellular leucine-rich repeat (eLRR) domain, a transmembrane domain and a cytoplasmic kinase domain play crucial roles in the recognition of pathogens in race-cultivar-

specific resistance (Dangl & Jones 2001) and in non-host general resistance (Nürnberger *et al.* 2004). The eLRR domain is a versatile scaffold that enables the eLRR proteins to interact with diverse biomolecules, including peptides, proteins and steroids (Wang *et al.* 2001; Russinova *et al.* 2004; Robatzek, Chinchilla & Boller 2006; Zipfel *et al.* 2006; Dunning *et al.* 2007).

All members of eLRR domain proteins are characterized by the distinct 24-residue LRR consensus sequence (Lxx-LxxLxxLxLxxNxLxGxIPxx) (Jones & Jones 1997; Kobe & Kajava 2001), Cys-containing LRR-flanking domains and several putative glycosylation sites (Kajava 1998). These characteristics are specific to plant eLRRs and differ in terms of length and composition of the LRRs from those found in other LRR subfamilies such as plant intracellular LRRs (Kobe & Kajava 2001; Forsthoefel *et al.* 2005).

Plant proteins with eLRR domains are categorized into four classes (van der Hoorn *et al.* 2005) based on their domain organization. The simplest class comprises of polygalacturonase inhibitor protein (PGIP)-like proteins, which are soluble and secretory and have only a single LRR domain with relatively limited number of repeats. They are glycoproteins located in plant cell walls that specifically inhibit fungal polygalacturonases (PGs) (Federici *et al.* 2006). The second class includes LRX-like proteins from *Arabidopsis thaliana*. Two members of LRX-like proteins, LRX1 and LRX2 are cell wall proteins required for root hair morphogenesis and constituted of a small eLRR domain fused to a variable C-terminal extensin-like domain (Baumberger, Ringli & Keller 2001; Baumberger *et al.* 2003). The third class is formed by the receptor-like proteins (RLPs) which contain an eLRR domain, a single transmembrane helix and a small cytosolic tail. This class is represented by the *Cf* family of tomato, whose members confer race-cultivar-specific resistance (van der Hoorn *et al.* 2005). The fourth and largest class is formed by the RLKs which contain an eLRR domain, a single membrane-spanning helix and a cytosolic kinase domain for signal transduction. This class includes proteins involved in non-host general

Correspondence: H.-M. Lam. Fax: +852 2603 5745; e-mail: honming@cuhk.edu.hk

defence such as the *Arabidopsis* flagellin receptor FLS2 (Gómez-Gómez, Bauer & Boller 2001) and receptors involved in race-cultivar-specific resistance such as Xa21 (Song *et al.* 1995) and Xa26 (Sun *et al.* 2004) from rice. In these R proteins, the signalling process that eventually leads to the activation of downstream defence effector genes is mainly accomplished by the LRR regions (Shanmugam 2005).

However, a more detailed analysis uncovered another distinct group of eLRR domain proteins. They are of simple structure (only a single LRR domain with relatively limited number of repeats) but exhibit strong sequence homology to the eLRR domain of some RLKs, such as the somatic embryogenesis receptor-like kinase (SERK) family proteins. Several members of this group of simple eLRR-type proteins were identified and they are implicated to play a role in plant defence response (Hipskind, Nicholson & Goldsbrough 1996; Tornero *et al.* 1996; Jung *et al.* 2004; Jacques *et al.* 2006; Jung & Hwang 2007).

For example, in sorghum, it is suggested that the SLRR protein may be involved in the protein-ligand binding and subsequent signal transduction pathway (Hipskind *et al.* 1996). The tomato LeLRP is a candidate molecule that may mediate recognition and interaction events taking place in the plant extracellular matrix under normal and/or pathogenesis-related conditions (Tornero *et al.* 1996). In tobacco, the *NtLRP1* gene is induced rapidly when hypersensitive response (HR) is initiated by the application of fungal elicitors or inoculation of bacteria or viruses. It may act as a modulator of HR to regulate the threshold of HR initiation (Jacques *et al.* 2006). In pepper, the CaLRR1 protein can interact with the pepper hypersensitive-induced response protein 1 (CaHIR1) and is specifically induced upon pathogen challenge and pathogen-associated molecular patterns (PAMPs) treatment (Jung & Hwang 2007). Co-transforming *CaLRR1* and *CaHIR1* into *A. thaliana* can compromise CaHIR1-induced HR. The authors propose that CaLRR1 functions as a negative regulator of CaHIR1-mediated cell death responses (Jung & Hwang 2007).

There are very few studies addressing the subcellular localization of this group of simple eLRR domain proteins. Transient expression and electron microscopic (EM) studies showed that *NtLRP1* proteins localize in the endoplasmic reticulum (ER), despite the absence of ER retention signals (Jacques *et al.* 2006).

In this work, we reported the cloning of a new member (OsLRR1) of this group of simple eLRR domain proteins from rice. We demonstrated that the OsLRR1 proteins enter the endosomal pathway, interacting with the HIR1 proteins, and will enhance defence response toward bacterial pathogen in transgenic *A. thaliana*.

MATERIALS AND METHODS

Plant materials, chemicals, reagents and primers

Arabidopsis thaliana wild-type Col-0 and *Oryza sativa* cultivar SN1033 are laboratory stocks. The *Pseudomonas*

syringae pv. *tomato* DC3000 (*Pst* DC3000) was a gift from Dr. C. Lo at University of Hong Kong. Enzymes and reagents for molecular studies were from Applied Biosystems (Foster City, CA, USA), Clontech Laboratories, Inc. (Palo Alto, CA, USA), Bio-Rad Laboratories (Hercules, CA, USA), Promega Biosciences (San Luis Obispo, CA, USA) and Roche Diagnostic Ltd. (Basel, Switzerland). DNA oligos were from Integrated DNA Technologies, Inc. (Coralville, IA, USA), Invitrogen Corp. (Carlsbad, CA, USA), and Tech Dragon Ltd. (Hong Kong). Chemicals for plant growth and tissue cultures were from Sigma-Aldrich Co. (St. Louis, MO, USA). Metro-mix200 soil for growth of *A. thaliana* was from Hummert International Supplier (Earth City, MO, USA). All primer sequences were given in Supporting Information Table S1.

RNA extraction, cDNA preparation, real-time PCR and Northern blot analysis

Procedures of RNA extraction, cDNA preparation and real-time PCR were performed as previously described (Ausubel *et al.* 1995; Sambrook & Russel 2001; Cheung *et al.* 2007). For real-time PCR, at least one biological repeat was performed using independent plant samples to ensure that the gene expression pattern was consistently observed. All reactions were set independently at least four times and at least three sets of consistent data were used for analysis. The expression levels of the *A. thaliana* *UBQ10* gene (*AtUBQ10*; GenBank accession number AY139999; Remans *et al.* 2008) and the *O. sativa* *UBQ5* gene (*OsUBQ5*; GenBank accession number AK061988; Jain *et al.* 2006) were used for normalization in *A. thaliana* and *O. sativa*, respectively. The relative gene expression was calculated using the $2^{-\Delta\Delta CT}$ method (Livak & Schmittgen 2001).

Northern blot analysis was performed as described (Ausubel *et al.* 1995; Sambrook & Russel 2001). Antisense single-stranded DNA probes were labelled with digoxigenin (DIG) (Roche, Mannheim, Germany) (Finckh, Lingenfelter & Myerson 1991).

Cloning of the full-length coding regions of OsLRR1 and OsHIR1 in rice, and their homologs in *A. thaliana*

A partial cDNA clone was obtained by random sequencing of cDNA libraries of pathogen-inoculated rice leaves (*Xa* lines inoculated with *Xanthomonas oryzae* pv. *oryzae* and *Pi* lines inoculated with *Magnaporthe grisea*; Cheung *et al.* 2007, 2008). 5' Rapid amplification of cDNA ends (5'-RACE) was employed to get the sequence information of the intact coding region (Supporting Information Table S1). For cloning of OsHIR1, the previously published sequence of CaHIR1 (Jung & Hwang 2007) was used to identify the rice homolog (GenBank accession number AF374475). The sequence information of the *AtLRR1* and *AtHIR1* clones was obtained from GenBank. Full-length coding regions were obtained by PCR of cDNA samples. Fidelity of DNA sequence was confirmed by sequencing.

Growth, pathogen inoculation and/or wounding treatments of rice and *A. thaliana*

Rice lines were grown on soil in a glasshouse under natural sunlight for 4 to 5 weeks. Pathogen inoculation was performed using the Chinese *X. oryzae* pv. *oryzae* (*Xoo*) race LN44 by a leaf-clipping method (Kauffman *et al.* 1973; Zhang *et al.* 1996; Cheung *et al.* 2007, 2008). The same procedure was used for wounding treatment except that the pathogen was replaced with water. For time-course experiments, the day 0 sample was collected before treatment. Other samples were collected at 2, 4 and 6 d after treatment at around the same time of day (between 0800 and 1000 h).

Arabidopsis thaliana were grown in a growth chamber (temperature 22–24 °C; relative humidity 70–80%; light intensity 80–120 $\mu\text{mol m}^{-2} \text{s}^{-1}$ on a 16 h : 8 h light-dark cycle). Preparation of the *Pst* DC3000 culture, inoculation and subsequent titre determination were performed as previously described (Uknes *et al.* 1992; Falk *et al.* 1999; Kim & Delaney 2002; Cheung *et al.* 2007, 2008).

Transformation, protoplasts preparation and subcellular localization studies

Transformation of *A. thaliana* and *O. sativa* was performed according to previous reports (Cheung *et al.* 2008). To express OsLRR1 and OsHIR1-GFP (GFP: green fluorescence protein) proteins in transgenic *A. thaliana*, the full-length cDNA clones were inserted into a binary vector (V7; Brears *et al.* 1993) and placed under the control of the cauliflower mosaic virus 35S promoter. *Agrobacterium*-mediated plant gene transfer was done as described previously (Bechtold & Pelletier 1998). T3 homozygous lines carrying a single insertion locus were used in this study. Constitutive expression of *OsLRR1* in *O. sativa* was controlled by a maize (*Zea mays*) ubiquitin promoter (Rooke, Byrne & Salgueiro 2000).

To transform into the tobacco BY-2 cells, recombinant constructs described above were first introduced into *Agrobacterium tumefaciens* (strain LBA4404) by a freeze-thaw method (Weigel & Glazebrook 2006). *Agrobacterium*-mediated transformation of the wild-type tobacco BY-2 cells was performed as described (Mayo, Gonzales & Mason 2006).

Protoplasts from OsLRR1-GFP transgenic BY-2 cells and root cells of OsHIR1-GFP transgenic *A. thaliana* were prepared as described (Miao & Jiang 2007; Yoo, Cho & Sheen 2007).

For confocal laser scanning microscopy studies, GFP (Ex: 488 nm; Em: 510–525 nm), Mito tracker (Ex: 554 nm; Em: 576 nm) and FM4-64 (e.g. 558 nm; Em: 734 nm) fluorescence was detected with an Olympus microscope (FV1000, Olympus, Tokyo, Japan). All samples were imaged with the 60 \times water or 40 \times objective lens. Pictures and videos were captured in Kahlman frame giving an average of four scans using an Olympus microscope FV1000 and the accompanying software FV10-ASW (version 01.07.02.02, Olympus).

Applications of inhibitors, elicitors and bacterial pathogens in subcellular localization studies

For brefeldin A (BFA) [B-6542, Sigma-Aldrich, stock solution at 2.5 mg mL⁻¹ in dimethyl sulphoxide (DMSO)] and Wortmannin (W1628, Sigma-Aldrich, stock solution at 1.0 mg mL⁻¹ in DMSO) treatments, stock solutions were added to 2- to 3-day-old suspension cultures at log phase to attain the final working concentrations (for BFA, 100 $\mu\text{g mL}^{-1}$; for Wortmannin, 16.5 μM) and were incubated for 30 min. Each drug treatment for confocal imaging was repeated at least three times and consistent results were observed.

Elicitor flg22 treatment (with a final concentration of 10 μM) was performed as described (Robatzek *et al.* 2006).

For bacterial treatments, *Pst* DC3000 was cultured as described above, 10 mL overnight culture [optical density (OD) 600 nm = 2.0] was centrifuged at 8000 g. The pellet was re-suspended in 4 mL 10 mM MgSO₄ and then added into BY-2 cell culture at 1:100 dilution. After incubating for 1 h at 26–28 °C, the cells were washed three times with fresh culture medium before subsequent microscopic analysis. Inoculation with *Escherichia coli* strain DH5 α was performed using the same procedure except that the bacterial cell pellet after centrifugation was re-suspended in Luria-Bertani medium.

FM4-64 PM localization and uptake study

The transgenic tobacco BY-2 suspension cell lines were first washed with Murashige & Skoog (MS) liquid medium, followed by the addition of FM4-64 (from a 12 mM stock) to 500 μL of cultured cells (in MS solution) to reach a final concentration of 12 μM .

When FM4-64 was used as a marker of the plasma membrane, samples were incubated on ice for less than 10 min. When FM4-64 was used as a marker of the endosomal pathway, samples were incubated on ice for 30 min. The FM4-64-treated cells were then washed with ice-cold MS medium three times and transferred onto a slide with the same medium for time-course observation and image collection using an Olympus microscope FV1000 and the software FV10-ASW (v01.07.02.02). The percentage of co-localization with endosomal vesicles was calculated by counting the co-localized signals and the total OsLRR1-GFP signals within the cells. At least 20 cells were used for calculation in each measurement.

Electron microscopy studies

Embedding and electron microscopy were performed as described (Lam *et al.* 2007) with some modifications. Fresh rice leaf discs were immediately frozen in a high-pressure freezing apparatus (EM PACT2; Leica, Wetzlar, Germany). For subsequent freeze substitution, the frozen samples were first kept at –85 °C for 16 h before gradually warming up to –50 °C over 5 h in the substitution medium [0.1% (w/v)

uranyl acetate in dry acetone] using an automated freeze-substitution unit (Leica). At -50°C , the medium was replaced with 100% ethanol for dehydration. The samples were then infiltrated stepwise with 33% HM20 and 66% HM20 in ethanol (1 h per step at -50°C), followed by substitution with 100% HM20 for 16 h at -50°C . The samples were then gradually warmed up to -35°C over 4 h and polymerized under ultraviolet light.

Immunolabelling of HM20 sections was done as described previously (Lam *et al.* 2007) using rabbit anti-OsLRR1 serum or mouse anti-OsHIR1 serum, respectively. Primary antibodies were detected by gold-coupled secondary antibodies. No non-specific binding was observed when the primary antibodies were left out (Supporting Information Fig. S1). Aqueous uranyl acetate/lead citrate post-stained sections were examined with the Hitachi H-7650 transmission electron microscope (Hitachi, Tokyo, Japan) operating at 80 kV.

Yeast two-hybrid experiments

Constructs fused to the activation domain (AD) and DNA-binding domain (BD) of the pGADT7-rec and pGBKT7 plasmid vectors were co-transformed into the yeast strain AH109 according to a simplified transformation protocol (Gietz *et al.* 1997). Selection of yeast cells containing both plasmids was done on synthetic dropout medium without leucine and tryptophan (SD-Leu-Trp) plates. After incubating for 3 to 4 d at 30°C , the yeast colonies were dotted onto SD agar plates without leucine, tryptophan, histidine, and adenine, and supplemented with 2 mg mL^{-1} 5-bromo-4-chloro-3-indolyl- α -D-galactopyranoside (SD-Leu-Trp-His-Ade/X- α -Gal). Other detailed procedures were described in the manufacturer's handbook (Yeast Protocols Handbook; PT3024-1; Clontech).

Protein extraction, antibodies and Western blot analysis

Total, membrane-bound and soluble proteins were separated using a modified fractionation method (Jiang & Rogers 1998; Cheung *et al.* 2007, 2008). For protein extraction from the culture medium, a trichloroacetic acid precipitation method was used (Guy, Philip & Tan 1994).

Primary antibodies (polyclonal) against the OsLRR1 protein were raised via a commercial service (Invitrogen) by injecting a synthetic peptide ('N'-CLSNFEKNPRLEGPE-'C') into rabbits. Primary antibodies (polyclonal) against the OsHIR1 protein were raised by injecting maltose-binding protein (MBP)-OsHIR1 fusion proteins expressed in *E. coli* into mice. Anti-glutathione S-transferase (GST) antibodies (G7781, Sigma Chemical Co.) and anti-MBP antibodies (M6295, Sigma Chemical Co.) were commercially available. Anti-rabbit or anti-mouse secondary antibodies conjugated to an alkaline phosphatase (provided in the Western Breeze Immunodetection Kit; WB7106; Invitrogen) were used for primary antibody recognition.

For Western blot analysis, the proteins were electrophoretically separated on an sodium dodecyl sulphate-polyacrylamide gel electrophoresis (SDS-PAGE) (4% stacking; 12.5% resolving) before being transferred to an activated polyvinylidene difluoride (PVDF) membrane pre-treated with absolute methanol for 5 min, and then to protein transfer buffer for 5 min, using the Bio-Rad Mini Trans-Blot Electrophoretic Transfer Cell (170-3930; Bio-Rad). The transfer, blocking (with Western Breeze blocking solution) and detection (using the Western Breeze Immunodetection Kit) procedures were performed according to manufacturer's manuals.

Expression in *E. coli* and *in vitro* pull-down

To express the target proteins in *E. coli*, the *OsLRR1* and *OsHIR1* cDNAs were cloned into pGEX-4T-1 (GE Healthcare, Chalfont St Giles, UK) and pMAL-c2 (New England Biolabs, Inc., Ipswich, MA, USA) vectors to form in-frame fusions with the GST or MBP coding sequences, respectively. After transforming the *E. coli* strain DE3, expression of the target proteins was induced by adding 0.5 mM isopropyl- β -D-thiogalactopyranoside (IPTG) to the growth medium. Protein purification was performed with the GST SpinTrap™ Purification Module (27-4570-03; GE Healthcare) or the SpinClean MBP Excellose Kit (23050, Mbio-tech, Seoul, Korea), following the procedures described in the user manuals.

For *in vitro* pull-down experiments, the GST fusions and the corresponding MBP fusions ($2.5\ \mu\text{g}$ each) were added to a final volume of $30\ \mu\text{L}$ and incubated with rotation at 4°C for 2 h. After adding $20\ \mu\text{L}$ of the anti-MBP magnetic beads (E8037S, New England Biolabs), the samples were mixed thoroughly and incubated at 4°C overnight with rotation. Interacting protein complexes were obtained using magnet and the supernatant was decanted. The beads were washed with phosphate buffered saline containing 0.1% Tween-20 with brief vortexing. The bead pellet was re-suspended in $40\ \mu\text{L}$ of 3 \times SDS sample loading buffer [$187.5\ \text{mM}$ Tris-HCl (pH6.8), 6% SDS, 30% glycerol, 150 mM dithiothreitol, 0.03% bromophenol blue, 2% β -mercaptoethanol] to elute the interacting proteins partners. The Western signal was detected using anti-GST antibodies (G7781, Sigma Chemical Co.) and anti-MBP antibodies (M6295, Sigma Chemical Co.).

Lactophenol-trypan blue staining

Micro-HR (spontaneous cell death) was detected using lactophenol-trypan blue staining as previously described (Koch & Slusarenko 1990).

RESULTS

OsLRR1 encodes a simple eLRR domain protein which is up-regulated upon pathogen challenging and wounding treatment

During a search for signalling components related to rice defence response, a partial cDNA clone encoding an eLRR

Figure 1. Structural domains, phylogenetic relationships, pathogen inoculation-induced and wounding induced expression pattern of OsLRR1 from rice. (a) Alignment of the amino acid sequences of OsLRR1 and somatic embryogenesis receptor-like kinase (SERK) (SERK family proteins). Both contain a signal peptide (SP), a leucine zipper (LZ) and a LRR domain with four leucine-rich repeats. SERK family proteins have an additional transmembrane domain (TM) and intracellular protein kinase domain (PK). (b) Sequence alignment of OsLRR1 and its homologs. Black boxes indicate the conserved amino acid residues found in three or more proteins in a given position. Underlined regions I, II and III were the position of the SP, LZ and LRR domains. Except SLRR that has five perfect LRR repeats, other members contain four perfect repeats. OsLRR1 (from rice; GenBank accession number AAO85403); LeLRP (from tomato; GenBank accession number CAA64565); AtLRR1 (from *Arabidopsis*; GenBank accession number AAG40341); NtLRP1 (from tobacco; GenBank accession number AAZ91738); CaLRR1 (from pepper; GenBank accession number AAN62015); SLRR (from sorghum; GenBank accession number AAC49559). The arrow indicates the possible cleavage site of the SP in OsLRR1. (c) Phylogenetic analysis of OsLRR1 and its homologs. Multiple-sequence alignment was performed using the ClustalW program (<http://www.ebi.ac.uk/clustalW/>). Unrooted phylogenetic tree was constructed with the MEGA4 program (Tamura *et al.* 2007). Tree topology was calculated by neighbour-joining method (Saitou & Nei 1987) and 1000 replicates were used for bootstrap test. (d) The mRNA and protein levels of OsLRR1 upon pathogen inoculation. Ten micrograms total RNA and 10 μ g total protein were loaded onto each lane. (e) The mRNA and protein levels of OsLRR1 upon wounding. Ten micrograms total RNA and 10 μ g total protein were loaded onto each lane. (f) Western blot analysis of OsLRR1 using fractionated protein samples of rice leaves. CS: soluble fraction; CM: membrane-associated fraction.

domain protein was identified by random sequencing of cDNA libraries of pathogen-inoculated rice leaves (see Materials and Methods). 5' RACE was employed to get the sequence information of the intact coding region (refer to Supporting Information Table S1). The *OsLRR1* cDNA clone encodes a simple eLRR domain protein (Fig. 1a), which is identical to an annotated LRR protein-like clone (GenBank accession number AAO85402). The corresponding gene is unique and located on rice chromosome 1.

Computational analysis of the OsLRR1 protein highlighted three successive domains, from N-terminus to C-terminus: a putative signal peptide, a leucine zipper (LZ) domain and an eLRR domain. The signalP 3.0 algorithm (Emanuelsson *et al.* 2007) predicted a signal peptide with a cleavage site after the 23rd amino acid. The LZ fits the consensus sequence compiled of repetitions of a group of seven amino acids starting with a leucine, Lxxxxxx (Landschulz, Johnson & McKnight 1988). There is an eLRR domain comprising four perfect repeats showing coincidence with the plant-specific consensus sequence: LxxLxxLxxLxLxxNxLxGxIPxx (Jones & Jones 1997; Kobe & Kajava 2001). OsLRR1 also contains two potential N-linked glycosylation sites at positions 77 and 125.

The OsLRR1 protein exhibits high similarity (from 48% to 82% identity) to homologs from dicots and monocots, including *A. thaliana*, sorghum (Hipskind *et al.* 1996), tomato (Tornerio *et al.* 1996), tobacco (Jacques *et al.* 2006) and pepper (Jung *et al.* 2004; Jung & Hwang 2007) (Fig. 1b). All of these eLRR domain proteins contain a single eLRR domain with 4–5 perfect repeats. Phylogenetic analysis (Fig. 1c) showed that OsLRR1 is grouped with two dicot homologs, the tomato LeLRP (82% identity spanning 191 residues) and the *Arabidopsis* AtLRR1 (78% identity spanning 208 residues), and is relatively distanced from the other branch consisted of sorghum SLRR (48% identity spanning 181 residues), tobacco NtLRP1 (53% identity spanning 200 residues) and pepper CaLRR1 (53% identity spanning 177 residues).

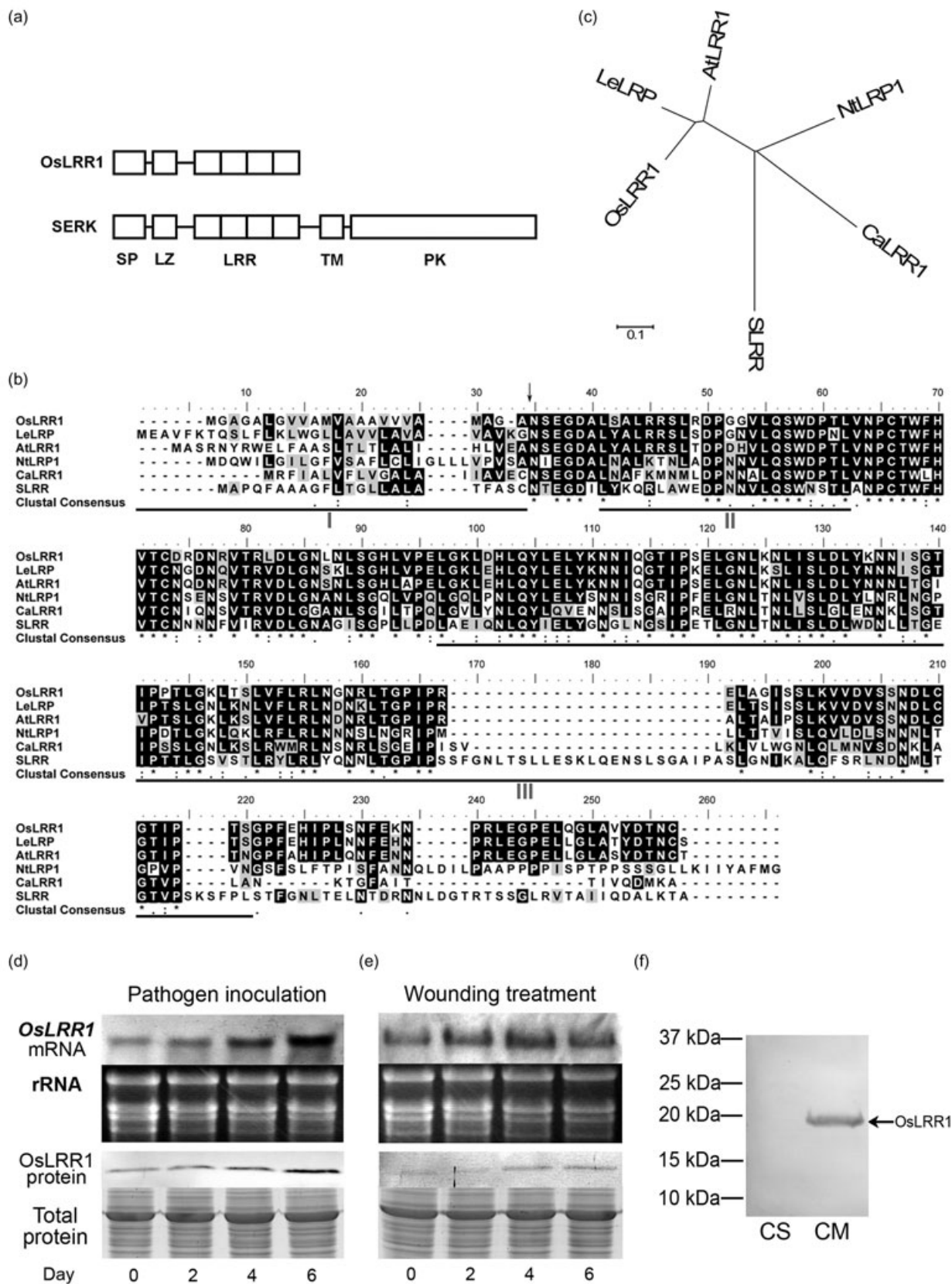
OsLRR1 also exhibits strong homology to the eLRR domains of several SERK proteins, including AtSERK1

(GenBank accession number NP_177328, 62% identity spanning 182 residues), AtBAK1 (GenBank accession number NP_567920, 64% identity spanning 168 residues) and OsSERK1 (GenBank accession number BAD86793, 59% identity spanning 197 residues). Comparing the protein structure of OsLRR1 with SERK proteins, they share common LZ and LRR motifs with relative high identity, but OsLRR1 lacks the transmembrane domain (TM) and the intracellular kinase domain present in SERK proteins (Fig. 1a).

To study the expression pattern of *OsLRR1*, Northern and Western blot were performed. Pathogen challenging using *Xoo* race LN44 can cause up-regulation of OsLRR1 both in mRNA and protein levels (Fig. 1d). Since many components of basal resistance are induced by wounding (Yoshimura *et al.* 1998; Cheung *et al.* 2007, 2008), the expression of OsLRR1 in response to wounding was also investigated by Northern and Western blot using leaf samples collected 2, 4 or 6 d after wounding treatment. It was observed that wounding could induce the expression of OsLRR1 at both mRNA and protein levels (Fig. 1e). Further studies using fractionated protein samples from untreated rice leaves showed that within the detection limit of the methodology used, OsLRR1 was found exclusively in the membrane-associated protein fraction (Fig. 1f).

OsLRR1 proteins enter the endosomal pathway

To precisely determine the subcellular localization of OsLRR1 proteins, we employed both confocal and EM analyses. In transgenic BY-2 cells expressing the OsLRR1-GFP fusion protein, most fluorescent signals were found on vesicles and exhibited a punctated pattern. Only a small portion of signals was found on the plasma membrane (Fig. 2a). The cytoplasmic organelles labelled by the OsLRR1-GFP fusion were not static but highly mobile within the cell (Supporting Information Video S1). These organelles moved to, along and away from the plasma membrane.



To elucidate the identity of these organelles, the BY-2 cells were treated with BFA and Wortmannin. BFA treatment will lead to aggregation of *trans*-Golgi network (TGN) due to the inhibition of the ARF1 GTPase and the subsequent blockage of the coat protein complex I (COPI)-mediated recycling pathway from the Golgi apparatus to the ER (Nebenführ, Ritzenthaler & Robinson 2002). BFA compartments formed by the accumulation of Golgi membranes in highly vesiculated clusters contain proteins localized on early endosomes. In OsLRR1-GFP transgenic BY-2 cells treated with BFA, a portion of fluorescent signals was found in BFA compartments (Fig. 2b), suggesting that at least some of the OsLRR1 proteins were localized in early endosomes. However, there were also fluorescent signals that were not aggregated, indicating other possible localizations. Wortmannin can cause late endosomes to dilate and form typical ring-like structures (visualized as multivesicular bodies (MVBs) (Tse *et al.* 2004). We showed that Wortmannin could induce the OsLRR1-GFP labelled MVBs to form small vacuoles and typical ring-like structures (Fig. 2c). Together, these findings suggest that the organelles labelled by OsLRR1-GFP are present in both early and late endosomes in BY-2 cells.

To further verify that the OsLRR1-GFP-labelled organelles are in the endosomal pathway, we performed uptake studies using FM4-64, a fluorescent styryl dye that is internalized via endocytosis from the plasma membrane

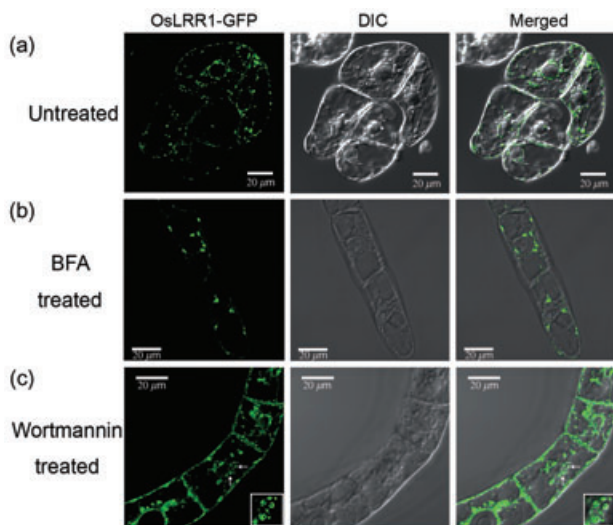


Figure 2. The effects of Brefeldin A (BFA) and Wortmannin on the localization of OsLRR1-GFP in transgenic tobacco BY-2 cells. The fluorescent signals of OsLRR1-GFP were observed in transgenic BY-2 cells without drug treatment (a), treated with BFA (b), or treated with Wortmannin (c). In untreated samples (a), OsLRR1-GFP gave punctuated signals. The localization of these signals was dynamic (see also Supporting Information Video S1). BFA treatment (b) could induce the formation of aggregated signals. Wortmannin treatment (c) resulted in signals in dilated organelles and ring-like structure (indicated by white arrows and magnified four-folds in the inset at the lower right-hand corner). DIC, differential interference contrast. Bars = 20 µm.

to the lytic vacuole (Emans, Zimmermann & Fischer 2002; Tse *et al.* 2004). The dye MitroTracker Orange CMTMRos that stains mitochondria was used as a negative control. MitroTracker signals did not co-localize with the signals from OsLRR1-GFP (Fig. 3a). In BY-2 cells expressing GFP only, the internalized FM4-64 was not co-localized with the GFP signals (Fig. 3b). Nonetheless, when BY-2 cells expressing OsLRR1-GFP were used, the signals of internalized FM4-64 largely co-localized with the fluorescent signals of OsLRR1-GFP proteins, indicated as yellow-coloured dots in the cytosol in the merged images (Fig. 3c). The percentage of co-localization was about 91%. A live image capture showed that most punctuated signals from FM4-64 and OsLRR1-GFP moved in unison within the cell as yellow-coloured dots, further indicating their co-localization (Supporting Information Video S2).

The deep orange colour of the plasma membrane in the merged images may be due to the relatively less amount of OsLRR1 proteins on plasma membrane. OsLRR1-GFP signals could also be observed on newly forming cell plate in cells undergoing mitosis (Fig. 3c, indicated by the white arrow). This provided an evidence to support the notion that some OsLRR1 proteins were localized on plasma membrane (Dhonukshe *et al.* 2006). Further experiments using protoplasts prepared from BY-2 cells expressing OsLRR1-GFP confirmed the co-localization of OsLRR1-GFP proteins and the internalized FM4-64 (Fig. 3d). The percentage of co-localization was about 84%.

To confirm the endosomal localization of the OsLRR1 protein, we performed EM studies using rice leaf samples and OsLRR1 specific antibodies. Detailed analysis showed that OsLRR1 proteins could be found on plasma membrane (Fig. 4a), clathrin-coated double-layered vesicles (Fig. 4b), clathrin-coated, tubular-vesicular-like early endosomes (Fig. 4c) and 500 nm-diameter double-layered late endosomes (Fig. 4d). The clathrin-coated vesicles could be responsible for the transportation of OsLRR1 proteins from the plasma membrane to the early endosomes. Therefore, the subcellular localization of OsLRR1 in native rice system deduced by EM studies was consistent with the confocal microscopic analysis using OsLRR1-GFP fusion proteins in transgenic BY-2 cells. A negative control of EM studies with only the secondary antibodies was shown in Supporting Information Fig. S1.

We also performed Western blot using concentrated culture medium of the transgenic BY-2 cell lines expressing OsLRR1-GFP and a rice suspension cell line. No OsLRR1-GFP or OsLRR1 could be detected in culture medium (Supporting Information Fig. S2). Therefore, most OsLRR1 proteins were recycled back to endosomes rather than secreted to the extracellular sap.

Using the transgenic BY-2 cells, we tested the possible effects on the subcellular localization of OsLRR1 by applying the elicitor flg22 (Robatzek *et al.* 2006) and incubating with bacteria (*E. coli* and *P. syringae*). However, we did not find an observable difference under these treatments (Supporting Information Fig. S3).

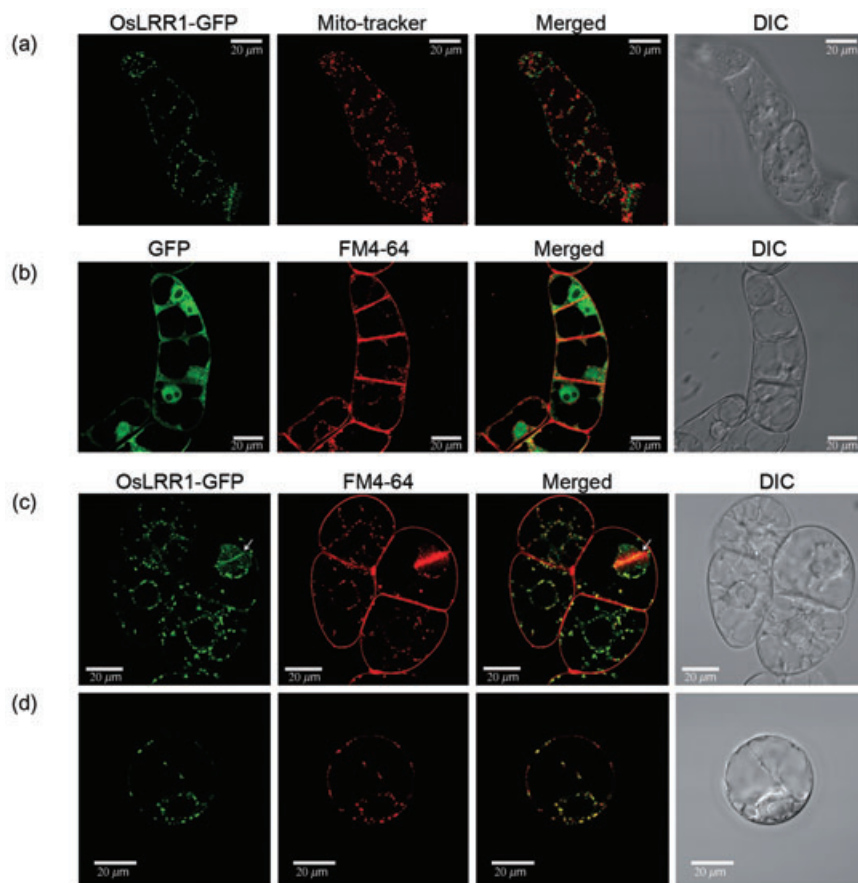


Figure 3. Co-localization of OsLRR1-GFP with marker dyes. The localization of fluorescent signals from OsLRR1-GFP (a, c, d) or free GFP (b) was tracked by using the marker dyes Mito-tracker (a; to mark mitochondria) or FM4-64 (b–d; to mark endosomes). Observations were done in intact cells (a–c) or protoplasts (d). Yellow-coloured dots in the merged images indicate co-localization of OsLRR1-GFP and FM4-64 in cytosol. These yellow dots were highly dynamic (see also Supporting Information Video S2). The white arrow indicates the position of a newly forming cell plate (plasma membrane in nature) in cells undergoing mitosis. The incubation time of Mito-tracker and FM4-64 was 10 min and 30 min, respectively. The duration of FM4-64 treatment was optimized to track the endosomal pathway. DIC, differential interference contrast. Bars = 20 μ m.

The OsLRR1 protein interacts with the plasma membrane-localized *O. sativa* hypersensitive-induced response protein 1 (OsHIR1)

One homolog of the OsLRR1 protein in pepper (*CaLRR1*) was previously shown to interact with the pepper hypersensitive-induced reaction protein 1 (*CaHIR1*) (Jung & Hwang 2007).

To test whether similar interaction exists in rice, the cDNA clones of *OsLRR1* and *OsHIR1* were cloned into both pGBKT7 and pGADT7-rec vectors. The *in vivo* interaction between OsLRR1 and OsHIR1 was demonstrated by the yeast two-hybrid method, using reciprocal AD and BD fusion constructs (Fig. 5a). Positive results were indicated by growth and blue colour on selective medium (SD-Leu-Trp-His-Ade) containing X- α -Gal.

Such protein–protein interaction was further verified by *in vitro* pull-down assays. OsLRR1 and OsHIR1 were fused to MBP and GST to make four recombinant constructs (Fig. 6). Free MBP and GST proteins were used as the negative control. Anti-MBP magnetic beads were used to pull down free MBP and MBP fusion proteins (Fig. 6a). When detected with anti-MBP antibody, protein bands corresponding to MBP-OsLRR1, MBP-OsHIR1 and free MBP were detected, indicating that the pull-down step was successful. Anti-GST antibody was used to detect protein bands in a duplicated blot (Fig. 6b). Protein bands of

GST-OsHIR1 and GST-OsLRR1 were only detected in samples containing MBP-OsLRR1 and MBP-OsHIR1, respectively. Together with the yeast two-hybrid results, the interaction between OsLRR1 and OsHIR1 was clearly demonstrated.

We further showed that such interaction is also conserved in other plants such as *A. thaliana*. The cDNA clones encoding *Arabidopsis* homologs of OsLRR1 and OsHIR1 were obtained, identified as AtLRR1 (GenBank accession number AF324989) and AtHIR1 (GenBank accession number AY114572), respectively. The interaction between AtLRR1 and AtHIR1 was very similar to their counterparts in rice (Fig. 5b).

Additional yeast two-hybrid experiments were performed to investigate the conservation of such protein–protein interactions using homologs. We successfully demonstrated that OsLRR1 and OsHIR1 could interact with AtHIR1 and AtLRR1, respectively (Fig. 5c,d). This is the first evidence to show the conserved interactions between LRR1 and HIR1 homologs from two different plant species.

The CaHIR1 protein possesses an N-myristoylation motif and a putative transmembrane motif that may be critical for its localization on plasma membrane (Jung & Hwang 2007). OsHIR1 also carries the N-myristoylation motif and the transmembrane domain at similar positions (Supporting Information Fig. S4). Although the predicted

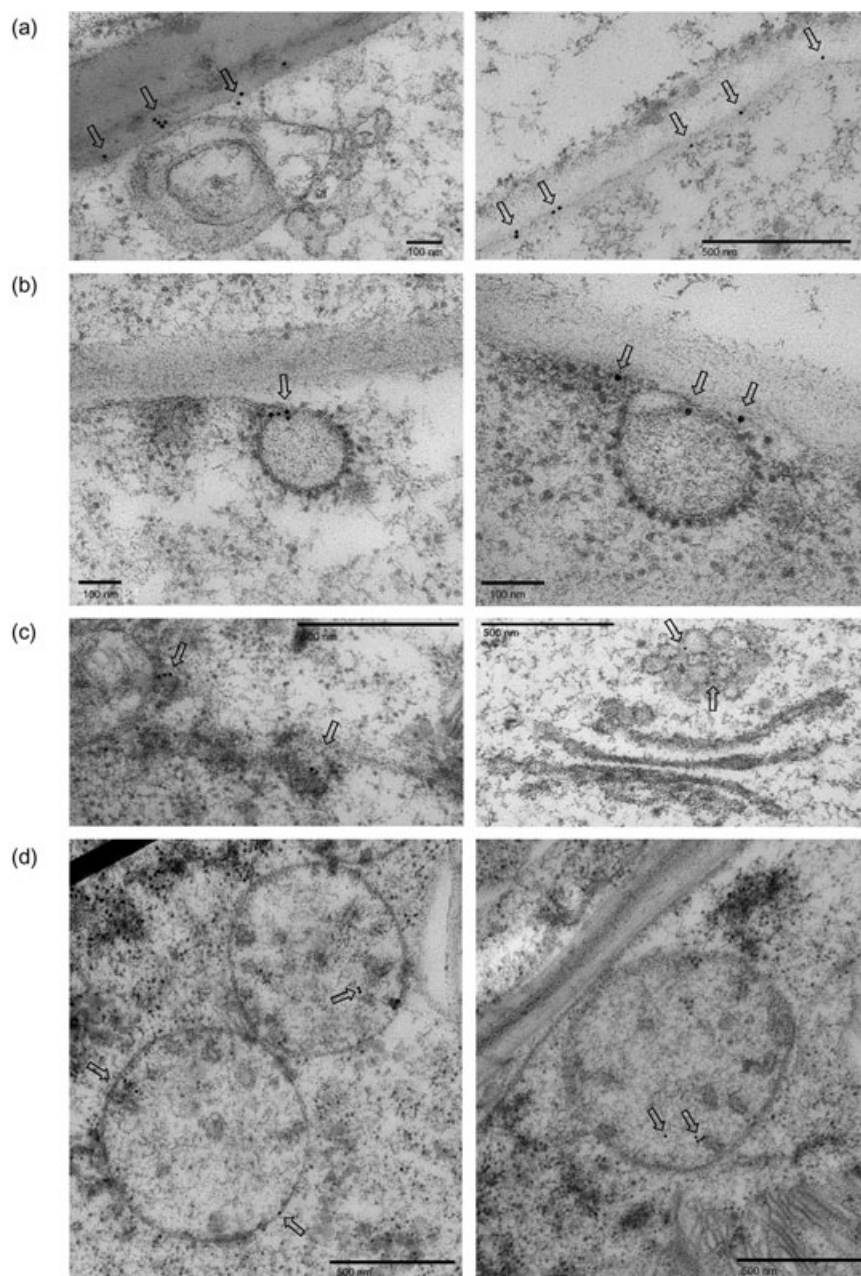


Figure 4. Immunogold electron-microscopic study of the localization of OsLRR1 proteins in cells of rice leaves. Ultra-thin sections prepared from high-pressure frozen/freeze-substituted rice leaves were immunogold-labelled with OsLRR1 antibodies. Arrows indicated the locations of gold particles presented on plasma membrane (a), clathrin-coated double-layered vesicles (b), clathrin-coated, tubular-vesicular-like early endosomes (c), and 500 nm-diameter double-layered multivesicular bodies (late endosomes). Two independent samples were shown in each panel. Magnification bars were given in each photo.

transmembrane domain of OsHIR1 is of a lower score (0.402 compared with 0.844 of CaHIR1), the relative high sequence homology (84% overall identity with CaHIR1; Supporting Information Fig. S4a) and the similar hydrophobicity topology (Supporting Information Fig. S4b) suggest that OsHIR1 may also localize to the plasma membrane.

Western blot analysis showed that OsHIR1 proteins, with a molecular weight ~31 kDa, were found in

membrane-associated protein fraction (Fig. 7a). Immunogold electron microscopy experiment was performed and the signals were mainly found on the plasma membrane (Fig. 7b). To further confirm the plasma membrane localization of OsHIR1, the OsHIR1-GFP construct was made and transferred into *A. thaliana*. The root of transgenic *A. thaliana* expressing the OsHIR1-GFP fusion protein was imaged using confocal laser scanning microscopy. The

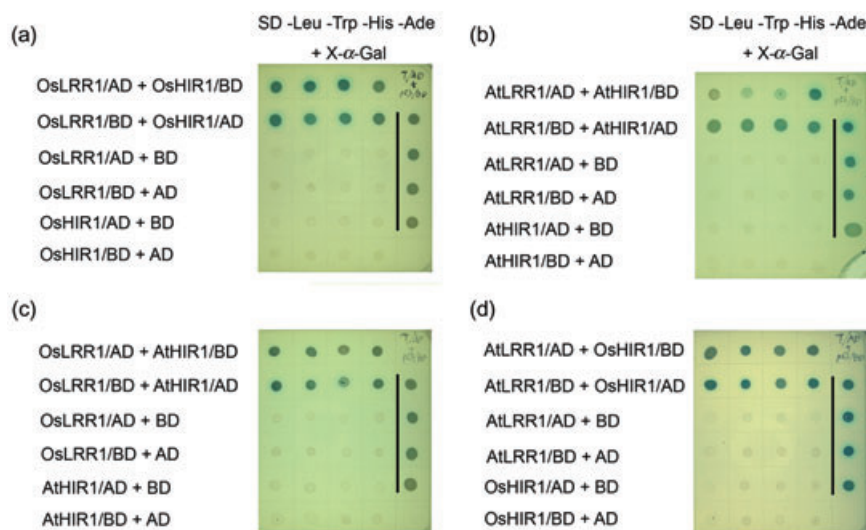


Figure 5. *In vivo* interactions of LRR1 and HIR1 proteins. The *in vivo* interactions of OsLRR1 versus OsHIR1 (a), AtLRR1 versus AtHIR1 (b), OsLRR1 versus AtHIR1 (c), and AtLRR1 versus OsHIR1 (d) were studied using a GAL4-based yeast two-hybrid system. The details were given in Materials and Methods. Empty vectors expressing just the AD or BD were used as the negative controls. The yeast colonies on the right side of the black line on each plate are the positive control included in the commercial kit.

fluorescent signals were detected on the plasma membrane (Fig. 7c). Protoplasts were prepared by digesting the root cells of the transgenic plants. Fluorescent signals of the fusion protein co-localized with the dye FM4-64 (Fig. 7d) (this dye could act as a marker for plasma membrane within 10 min of incubation with plant cells when placed on ice [Lam *et al.* 2007]). The subcellular localization of OsHIR1 proteins was mainly on the plasma membrane, but the signal pattern seemed to be punctated.

Ectopic expression of *OsLRR1* in transgenic *A. thaliana* enhances resistance to *P. syringae* pv. *tomato* DC3000 (*Pst* DC3000)

The possible involvement of some OsLRR1 homologs in plant defence response (see Introduction), together with the highly conserved OsLRR1 and OsHIR1 homologs and their interactions in *A. thaliana* (Fig. 5) prompted us to perform a rapid gain-of-function test using transgenic *A.*

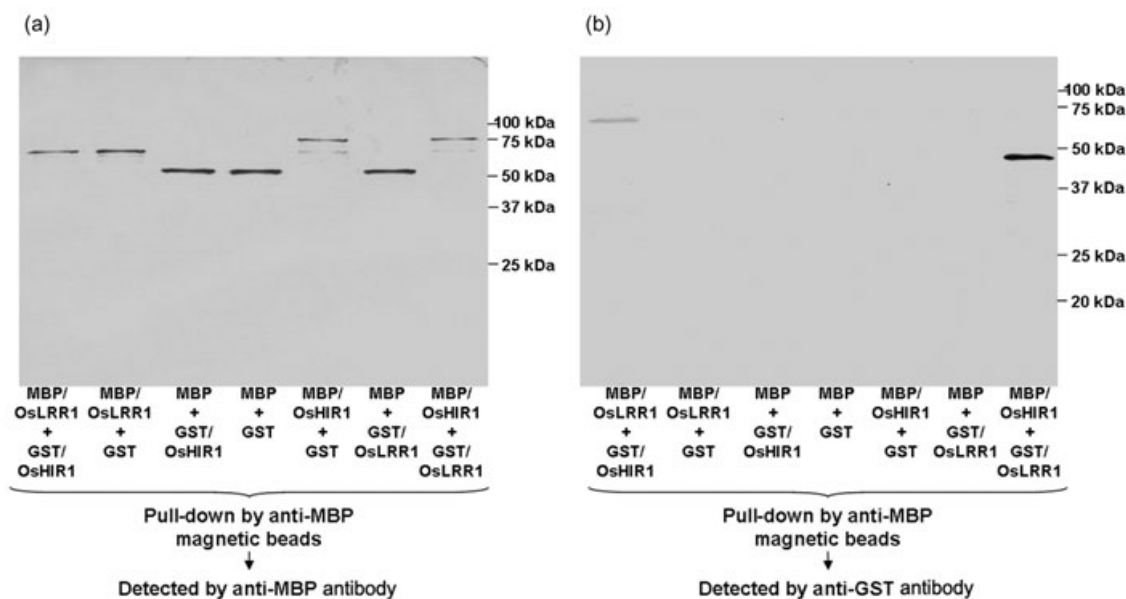


Figure 6. *In vitro* pull-down of the OsLRR1 and OsHIR1 proteins. Recombinant proteins of OsLRR1 or OsHIR1 fused to maltose-binding protein (MBP) or glutathione S-transferase (GST) were expressed in the *Escherichia coli* strain DE3. Free MBP and GST were also produced and used as the negative controls. Different combinations of purified proteins were mixed as indicated in the figure. All protein mixtures were pulled down by anti-MBP magnetic beads. Duplicated blots were made and detected with anti-MBP (a) or anti-GST (b) antibodies. Signals detected in panel (a) or (b) indicate successful pull-down by anti-MBP beads or positive protein–protein interactions, respectively.

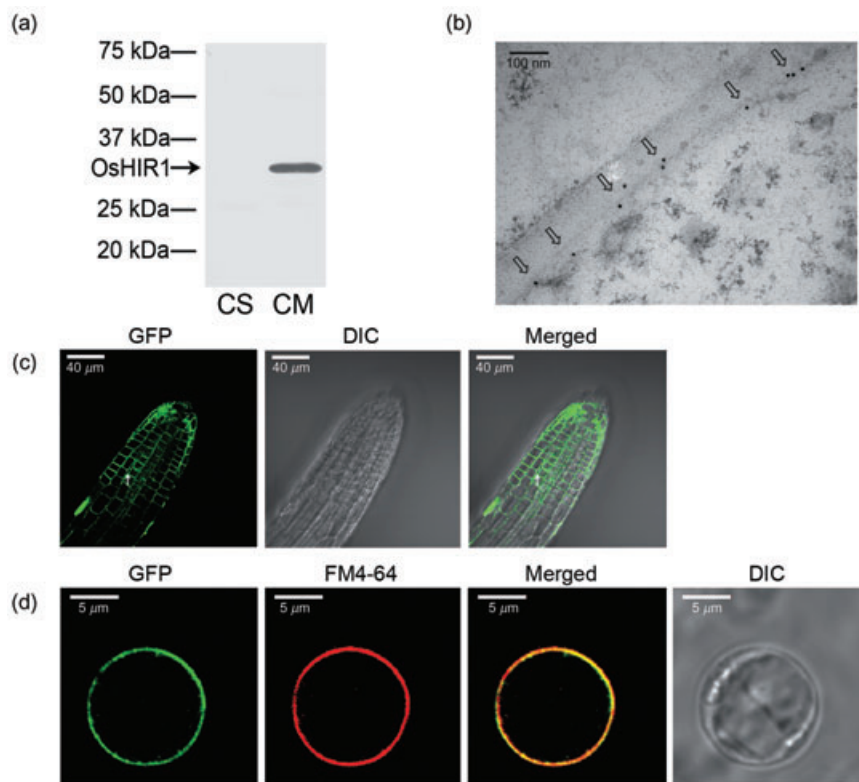


Figure 7. Subcellular localization of OsHIR1 in rice and OsHIR1-GFP in transgenic *Arabidopsis thaliana*. (a) Western blot analysis of OsHIR1 using fractionated protein samples of rice leaves. (b) Immunogold EM detection of OsHIR1 proteins. Arrows indicate position of gold particles. Bars = 100 nm. (c) Confocal microscopic studies of OsHIR1-GFP signals in root cells of transgenic *A. thaliana*. The white arrow indicates the apoplast gap between root cells. Bars = 40 μm . (d) Co-localization of OsHIR1-GFP signals with FM4-64. Protoplasts were prepared by digesting root cells [same construct as shown in (c)] with cellulase and pectinase. Detection of FM4-64 was performed within 10 min after incubation with the protoplasts. This timing is to optimize the utilization of FM6-64 as a plasma membrane marker. CS, soluble fraction; CM, membrane-associated fraction; DIC, differential interference contrast. Bars = 5 μm .

thaliana. *OsLRR1* was ectopically expressed in transgenic *A. thaliana*. When the pathogenic bacterium *Pst* DC3000 was inoculated onto Col-0 (wild-type *A. thaliana* parent) or *A. thaliana* transformed with the empty vector cassette, disease symptoms (yellowing and necrosis) gradually appeared (Fig. 8a). Such symptoms were much alleviated in transgenic lines expressing *OsLRR1*. Consistently, all transgenic lines also accumulated a lower titre of pathogens when compared with Col-0 and the empty vector control (Fig. 8b).

The expression of three defence marker genes (*PR1* and *PR2* for salicylic acid (SA) pathway; *PDF1.2* for jasmonic acid (JA) and ethylene (ET) pathways) was monitored in both mock- (Fig. 8c) and pathogen-inoculated (Fig. 8d) plant samples. In mock-treated plants, the expression levels of *PR1*, *PR2* and *PDF1.2* were elevated in transgenic plants when compared with Col-0 and transgenic plants with empty vector cassette. Upon pathogen inoculation, the expression levels of *PR1*, *PR2* and *PDF1.2* were up-regulated in Col-0 and empty vector construct. However, such up-regulation was much more prominent in transgenic plants expressing *OsLRR1*.

Although the uninoculated transgenic plants exhibited normal growth phenotype without pathogen attack, a very mild spontaneous micro-lesion was observed by staining with lactophenol-trypan blue (Supporting Information Fig. S5). This result provided a further support for the involvement of *OsLRR1* in plant defence response.

Overexpression of *OsLRR1* in *O. sativa* could enhance *PR* genes expression but not adequate to cause resistance to the pathogen *X. oryzae* pv. *oryzae*

We also constructed transgenic rice lines overexpressing *OsLRR1*. Expression of defence marker genes *PR1* and *PBZ1* were found to be enhanced when compared with the untransformed control (Supporting Information Fig. S6). However, when inoculated with a rice bacterial pathogen, *X. oryzae* pv. *oryzae* (*Xoo*), the transgenic lines did not reveal a significant protection (Supporting Information Fig. S7).

DISCUSSION

The proteins contain LRR motifs that are often involved in protein–protein interactions and are confined predominantly to eukaryotes (Kobe & Kajava 2001). In plants, two subfamilies of LRR domains are present: the extracellular plant-specific subfamily and the intracellular cysteine-containing subfamily. The LRR motif of *OsLRR1* structurally belongs to the plant-specific, extracellular LRR type.

Detailed analysis of the components of *OsLRR1* and its homologs reveals a unique group of simple eLRR domain proteins with a single LRR domain constituted of limited number of repeats and exhibited high homology to RLKs. Previous studies of these *OsLRR1* homologs implicated that

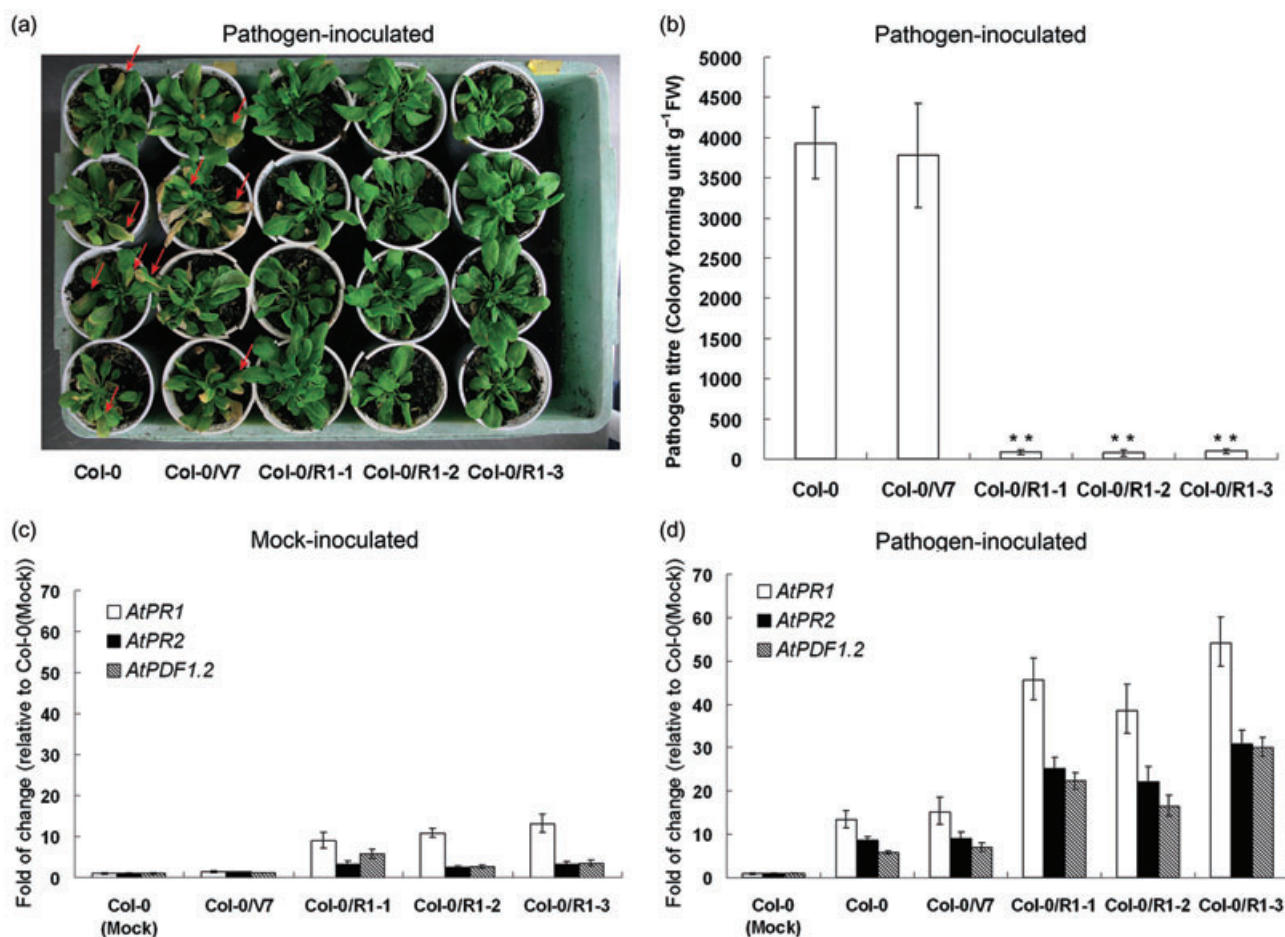


Figure 8. Pathogen inoculation test of transgenic *Arabidopsis thaliana* expressing OsLRR1. Six-week-old seedlings of transgenic *A. thaliana* seedlings from wild-type parent (Col-0), empty vector control (Col-0/V7) and three independent transgenic lines expressing OsLRR1 (Col-0/R1-1, Col-0/R1-2, Col-0/R1-3) were challenged with *Pseudomonas syringae* pv. *tomato* DC3000 (*Pst* DC3000) in a concentration of 10^8 colony forming units mL^{-1} in 10 mM MgSO_4 supplemented with 0.02% (v/v) Silwet L-77, via a dipping method. Disease symptoms (a) and pathogen titres (b) were observed and recorded 3 d after inoculation. Pathogen titres were measured using rosette leaves. ** indicates that the mean difference (compared to wild type and vector only) is significant at $P < 0.01$ level. The expression of defence marker genes in seedlings without (c) or with (d) *Pst* DC3000 inoculation was compared using real-time PCR of reverse-transcribed RNA samples. Relative expression levels of *PR1*, *PR2* and *PDF1.2* in each line were compared with the mock-inoculated wild-type parent Col-0 (expression level set to 1).

some members of this group of simple eLRRs may be involved in defence response (Hipskind *et al.* 1996; Tornero *et al.* 1996; Jung *et al.* 2004) or suppression of HR (Jacques *et al.* 2006; Jung & Hwang 2007). No direct proof of their functions in enhancing disease resistance was reported. This group of simple eLRR domain proteins is predicted to enter the secretory pathway due to the presence of a signal peptide and the absence of organelle retention signals. However, the subcellular distribution was only determined for one member of this group (NtLRP1) and the result suggests ER localization (Jacques *et al.* 2006). The role of NtLRP1 in plant defence response and the related importance of ER localization have not been thoroughly addressed.

Determination of the subcellular localization and trafficking of a regulatory protein often leads to new insights of its functions. To achieve a more definite answer to the trafficking pathway of the OsLRR1 protein, we validated our

results by several experimental approaches including confocal microscopy, electron microscopy and utilization of organelle-specific drugs. All results lead to the conclusion that OsLRR1 will enter the endosomal pathway. The OsLRR1 proteins could be found on plasma membrane, clathrin-coated vesicles, early endosome and late endosome. They co-localized and trafficked together with markers of the endosomal pathway.

The result of the endosomal localization of OsLRR1 is intuitive. Classical models of signal transduction cascades are based on the assumption that only the cell surface localized receptor pool is functionally relevant and downstream signalling components are freely accessible by diffusion (Geldner & Robatzek 2008). However, growing evidences show that subcellular trafficking of cell surface receptors is an integral part of signal transduction cascades. The confirmed endocytic processes in plants include the constitutive

RLK internalization (Shah *et al.* 2002; Russinova *et al.* 2004; Gifford *et al.* 2005) and the ligand-mediated receptor endocytosis (Robatzek *et al.* 2006). A plant cell membrane receptor, FLS2, functions to recognize a bacterial PAMP and exhibits ligand-induced endocytosis, providing evidence to show that endocytosis and signalling function are coupled (Robatzek *et al.* 2006). Due to the strong sequence and structural homology between the extracellular portion of these RLKs and the simple eLRR domain protein OsLRR1, together with the observation that OsLRR1 can enter the endosomal pathway, we speculate that the eLRR domain of these RLKs may somehow contribute to the internalization process.

No prior pathogen or elicitor challenges are needed to induce OsLRR1 proteins to enter the endosomal pathway. The behaviour of constitutive endocytic trafficking of OsLRR1 is different from ligand-induced endocytosis such as in the case of FLS2 (Robatzek *et al.* 2006). On the other hand, it mimics the case of the BRASSINOSTEROID INSENSITIVE1 (BRI1) [a RLK responsible for the perception of brassinosteroid (BR)] (Geldner *et al.* 2007). BRI1 proteins are constitutively present in both plasma membrane and endosomes to fulfil the function of BR signalling.

The subsequent question to address is the possible roles of OsLRR1 in plant defence response. Both the mRNA and protein levels of OsLRR1 were induced by pathogen challenge and wounding treatment, suggesting a close relationship between OsLRR1 levels and disease resistance. In rice, while some *R* genes are induced by wounding (e.g. *Xal1*; Yoshimura *et al.* 1998), other wounding inducible genes were implicated to participate in basal defence response (Cheung *et al.* 2007, 2008). We speculate that OsLRR1 may take part in the surveillance mechanism monitoring the presence of pathogens and relays the signals to trigger defence response. The presence of high levels of OsLRR1 may also help to enhance the defence response, since both the basal and pathogen-induced expression of defence marker genes were found to be at a higher level in transgenic *A. thaliana* ectopically expressing OsLRR1.

Another approach to dissect the function of OsLRR1 was to identify its interacting protein partner. It was reported that the OsLRR1 homolog in pepper (CaLRR1) can interact with the pepper hypersensitive-induced response protein 1 (CaHIR1). CaHIR1 plays an important role in HR (Jung & Hwang 2007). The involvement of HIR proteins in HR was also reported in other plants such as maize and barley (Nadimpalli *et al.* 2000; Rostoks *et al.* 2003). The *HIR* genes were differentially expressed in plant leaves during the development of spontaneous micro-HR lesions (Nadimpalli *et al.* 2000; Xiao, Tang & Zhou 2001; Rostoks *et al.* 2003). The HIR proteins belong to the PID (proliferation, ion and death) superfamily. Expression studies reveal that they are associated with localized host cell death and disease resistance response in maize and barley plants (Nadimpalli *et al.* 2000; Rostoks *et al.* 2003).

In a previous proteomic study, OsHIR1 protein was found in the plasma membrane fraction and its expression was up-regulated when challenged with the bacterial

pathogen *Xoo* (Chen *et al.* 2007). Using Western blot analysis and detailed microscopic studies, we showed that most OsHIR1 and some OsLRR1 proteins were localized on plasma membrane. We also provided strong evidence to show the interaction between OsLRR1 and OsHIR1 via both *in vivo* and *in vitro* assays. Furthermore, the interactions between LRR1 and HIR1 homologs are highly conserved in different plant species. Successful cross-species interactions between LRR1 and HIR1 proteins from rice and *A. thaliana* were clearly demonstrated.

Just like CaHIR1, both OsHIR1 and AtHIR1 were predicted to carry a transmembrane domain. Although the predicted transmembrane domain of OsHIR1 is of a relative low score (0.402 compared with 0.844 of CaHIR1 and 0.940 of AtHIR1), the relative high sequence homology (84% overall identity with CaHIR1 and 86% overall identity with AtHIR1) and the similar hydrophobicity topology suggest that this transmembrane domain may be conserved. Such transmembrane domain in HIR1 proteins may be important in their interaction with LRR1 proteins to initiate the downstream signal transduction pathway.

To further show the function of OsLRR1, transgenic *A. thaliana* ectopically expressing OsLRR1 was constructed. The protective effects of OsLRR1 were shown by the alleviated disease symptoms, lowering of pathogen titre in plant tissues and higher expression of defence marker genes. The observation that OsLRR1 from rice could enhance defence response in *A. thaliana* suggests the presence of a conserved defence mechanism in both monocots and dicots. It is consistent with the observed interaction between OsLRR1 and AtHIR1 proteins. It is interesting to observe that ectopic expression of *OsLRR1* in *A. thaliana* could induce expression of defence marker genes in both SA and JA pathways. For resistance toward the biotrophic pathogen *Pst* DC3000, the SA pathway plays dominant roles (Spoel, Johnson & Dong 2007). Expression of OsLRR1 may strengthen the defence response before and after pathogen attacks, leading to enhanced disease resistance. The induction of JA and ET pathway hints that OsLRR1 could also be involved in the defence against necrotrophic pathogens (Spoel *et al.* 2007).

The effects of expressing OsLRR1 in transgenic *A. thaliana* reported in this study are apparently different from the results of CaLRR1 (Jung & Hwang 2007). The *AtLRR1* gene is induced by incompatible pathogen and methyl jasmonate and is grouped under disease-resistance genes (Schenk *et al.* 2003; Li *et al.* 2006). *AtLRR1* is phylogenetically more close to OsLRR1 than CaLRR1. CaLRR1 and NtLRP1 are in the same cluster and both suppress HR (Jacques *et al.* 2006; Jung & Hwang 2007). They are distinct from the cluster containing *AtLRR1* and *OsLRR1*. The percentage of identity among the three homologs are OsLRR1 versus *AtLRR1* (78% spanning 208 residues), OsLRR1 versus CaLRR1 (53% spanning 177 residues) and *AtLRR1* versus CaLRR1 (57% spanning 177 residues). Moreover, we have demonstrated the conserved interaction between OsLRR1 and AtHIR1, while the interaction between CaLRR1 and AtHIR1 remains unproven. Overexpressing CaLRR1 in transgenic *A. thaliana* caused a

repression of *PR* gene expressions (Jung & Hwang 2007), while overexpressing OsLRR1 led to an increase in the basal level of *PR* gene transcripts. These differences may explain the opposite effects of expressing OsLRR1 and CaLRR1 on disease resistance in transgenic *A. thaliana*.

We also constructed transgenic rice lines overexpressing *OsLRR1*. Expression of defence marker genes *PRI* and *PBZI* were found to be enhanced when compared with the untransformed control. However, when inoculated with a rice bacterial pathogen, *X. oryzae* pv. *oryzae* (*Xoo*), the transgenic lines did not reveal a significant protection. This implies that overexpression of *OsLRR1* alone just led to a mild defence response, but this mechanism alone was not sufficient to cause resistance to bacterial blight.

In summary, we provided first experimental evidence to demonstrate the subcellular localization and trafficking of a novel simple eLRR domain protein OsLRR1 protein in the endosomal pathway. Since some eLRR domain containing RLKs also enter the endosomal pathway, further studies of the eLRR domain will be informative to the understanding of the underlying internalization process. The highly conserved interaction between LRR1 and HIR1 homologs provided evidence to show that such interaction is a common mechanism in the defence response of both monocots and dicots.

ACKNOWLEDGMENTS

This work was supported by the Hong Kong RGC General Research Fund CUHK467608 (to H.-M.L.), the Hong Kong UGC AoE Plant & Agricultural Biotechnology Project AoE-B-07/09 and the SHARF Grant (to H.-M.L. and S.S.-M.S.). Prof. C. Lo (Hong Kong Univ.) and Prof. Yiji Xia (Donald Danforth Plant Science Center, USA) kindly provided the pathogen strain *P. syringae* pv. *tomato* DC3000 and the elicitor flg22, respectively. Technical supports by Y. Shen, N.-Y. Zeng, W.-K. Kwok and S.-W. Tong (Chinese Univ. of Hong Kong), Y. Fu (Chinese National Rice Institute) and Q. Liu (Yangzhou University) are also highly appreciated. We also thank the critical reading of this manuscript by J. He (Chinese Univ. of Hong Kong).

REFERENCES

Ausubel F.M., Brent R., Kingston R.E., Moore D.D., Seidman J.G., Smith J.A. & Struhl K. (1995) Phenol/SDS method for plant RNA preparation. *Current Protocols in Molecular Biology*, Vol. 1. John Wiley & Sons, Inc., New York, UK, pp. 43.1–4.

Baumberger N., Ringli C. & Keller B. (2001) The chimeric leucine-rich repeat/extensin cell wall protein LRX1 is required for root hair morphogenesis in *Arabidopsis thaliana*. *Genes & Development* **15**, 1128–1139.

Baumberger N., Doesseger B., Guyot R., *et al.* (2003) Whole-genome comparison of leucine-rich repeat extensins in *Arabidopsis* and rice. A conserved family of cell wall proteins form a vegetative and a reproductive clade. *Plant Physiology* **131**, 1313–1326.

Bechtold N. & Pelletier G. (1998) In planta, *Agrobacterium*-mediated transformation of adult *Arabidopsis* 7 plants by vacuum infiltration. *Methods in Molecular Biology* **82**, 259–266.

Brears T., Liu C., Knight T.J. & Coruzzi G.M. (1993) Ectopic over-expression of asparagine synthetase in transgenic tobacco. *Plant Physiology* **103**, 1285–1290.

Chen F., Yuan Y., Li Q. & He Z. (2007) Proteomic analysis of rice plasma membrane reveals proteins involved in early defense response to bacterial blight. *Proteomics* **7**, 1529–1539.

Cheung M.Y., Zeng N.Y., Tong S.W., Li F.W., Zhao K.J., Zhang Q., Sun S.S. & Lam H.M. (2007) Expression of a RING-HC protein from rice improves resistance to *Pseudomonas syringae* pv. *tomato* DC3000 in transgenic *Arabidopsis thaliana*. *Journal of Experimental Botany* **58**, 4147–4159.

Cheung M.Y., Zeng N.Y., Tong S.W., *et al.* (2008) Constitutive expression of a rice GTPase-activating protein induces defense responses. *New Phytologist* **179**, 530–545.

Dangl J.L. & Jones J.D. (2001) Plant pathogens and integrated defence responses to infection. *Nature* **411**, 826–833.

Dhonukshe P., Baluska F., Schlicht M., Hlavacka A., Samaj J., Friml J. & Gadella T.W. Jr. (2006) Endocytosis of cell surface material mediates cell plate formation during plant cytokinesis. *Developmental Cell* **10**, 137–150.

Dunning F.M., Sun W., Jansen K.L., Helft L. & Bent A.F. (2007) Identification and mutational analysis of *Arabidopsis* FLS2 leucine-rich repeat domain residues that contribute to flagellin perception. *The Plant Cell* **19**, 3297–3313.

Emans N., Zimmermann S. & Fischer R. (2002) Uptake of a fluorescent marker in plant cells is sensitive to brefeldin A and wortmannin. *The Plant Cell* **14**, 71–86.

Emanuelsson O., Brunak S., von Heijne G. & Nielsen H. (2007) Locating proteins in the cell using TargetP, SignalP and related tools. *Nature Protocol* **2**, 953–971.

Falk A., Feys B.J., Frost L.N., Jones J.D., Daniels M.J. & Parker J.E. (1999) EDS1, an essential component of *R* gene-mediated disease resistance in *Arabidopsis* has homology to eukaryotic lipases. *Proceedings of the National Academy of Sciences of the United States of America* **96**, 3292–3297.

Federici L., Di Matteo A., Fernandez-Recio J., Tsernoglou D. & Cervone F. (2006) Polygalacturonase inhibiting proteins: players in plant innate immunity? *Trends in Plant Science* **11**, 65–70.

Finckh U., Lingenfelter P.A. & Myerson D. (1991) Producing single-stranded DNA probes with the *Taq* DNA polymerase: a high yield protocol. *Biotechniques* **10**, 35–38.

Forsthoefel N.R., Cutler K., Port M.D., Yamamoto T. & Vernon D.M. (2005) PIRLS: a novel class of plant intracellular leucine-rich repeat proteins. *Plant Cell Physiology* **46**, 913–922.

Geldner N. & Robatzek S. (2008) Plant receptors go endosomal: a moving view on signal transduction. *Plant Physiology* **147**, 1565–1574.

Geldner N., Hyman D.L., Wang X., Schumacher K. & Chory J. (2007) Endosomal signaling of plant steroid receptor kinase BRI1. *Genes & Development* **21**, 1598–1602.

Gietz R.D., Triggs-Raine B., Robbins A., Graham K.C. & Woods R.A. (1997) Identification of proteins that interact with a protein of interest: applications of the yeast two-hybrid system. *Molecular and Cellular Biochemistry* **172**, 67–79.

Gifford M.L., Robertson F.C., Soares D.C. & Ingram G.C. (2005) *ARABIDOPSIS* CRINKLY4 function, internalization, and turnover are dependent on the extracellular crinkly repeat domain. *The Plant Cell* **17**, 1154–1166.

Gómez-Gómez L., Bauer Z. & Boller T. (2001) Both the extracellular leucine-rich repeat domain and the kinase activity of FLS2 are required for flagellin binding and signaling in *Arabidopsis*. *The Plant Cell* **13**, 1155–1163.

Guy G.R., Philip R. & Tan Y.H. (1994) Analysis of cellular phosphoproteins by two-dimensional gel electrophoresis: applications for cell signaling in normal and cancer cells. *Electrophoresis* **15**, 417–440.

- Hipskind J.D., Nicholson R.L. & Goldsbrough P.B. (1996) Isolation of a cDNA encoding a novel leucine-rich repeat motif from *Sorghum bicolor* inoculated with fungi. *Molecular Plant-Microbe Interactions* **9**, 819–825.
- van der Hoorn R.A., Wulff B.B., Rivas S., Durrant M.C., van der Ploeg A., de Wit P.J. & Jones J.D. (2005) Structure-function analysis of cf-9, a receptor-like protein with extracytoplasmic leucine-rich repeats. *The Plant Cell* **17**, 1000–1015.
- Jacques A., Ghannam A., Erhardt M., de Ruffray P., Baillieux F. & Kauffmann S. (2006) NtLRP1, a tobacco leucine-rich repeat gene with a possible role as a modulator of the hypersensitive response. *Molecular Plant-Microbe Interactions* **19**, 747–757.
- Jain M., Nijhawan A., Tyagi A.K. & Khurana J.P. (2006) Validation of housekeeping genes as internal control for studying gene expression in rice by quantitative real-time PCR. *Biochemical and Biophysical Research Communications* **345**, 646–651.
- Jiang L. & Rogers J.C. (1998) Integral membrane protein sorting to vacuoles in plant cells: evidence for two pathways. *Journal of Cell Biology* **143**, 1183–1199.
- Jones D.A. & Jones J.D.G. (1997) The role of leucine rich repeat proteins in plant defenses. *Advances in Botanical Research* **24**, 89–167.
- Jung E.H., Jung H.W., Lee S.C., Han S.W., Heu S. & Hwang B.K. (2004) Identification of a novel pathogen-induced gene encoding a leucine-rich repeat protein expressed in phloem cells of *Capsicum annuum*. *Biochimica et Biophysica Acta* **1676**, 211–222.
- Jung H.W. & Hwang B.K. (2007) The leucine-rich repeat (LRR) protein, CaLRR1, interacts with the hypersensitive induced reaction (HIR) protein, CaHIR1, and suppresses cell death induced by the CaHIR1 protein. *Molecular Plant Pathology* **8**, 503–514.
- Kajava A.V. (1998) Structural diversity of leucine-rich repeat proteins. *Journal of Molecular Biology* **277**, 519–527.
- Kauffman H.E., Reddy A.P.K., Hsieh S.P.Y. & Merca S.D. (1973) An improved technique for evaluating resistance to rice varieties of *Xanthomonas oryzae*. *Plant Disease Reporter* **57**, 537–541.
- Kim H.S. & Delaney T.P. (2002) Arabidopsis SON1 is an F-box protein that regulates a novel induced defense response independent of both salicylic acid and systemic acquired resistance. *The Plant Cell* **14**, 1469–1482.
- Kobe B. & Kajava A.V. (2001) The leucine-rich repeat as a protein recognition motif. *Current Opinion in Structural Biology* **11**, 725–732.
- Koch E. & Slusarenko A. (1990) *Arabidopsis* is susceptible to infection by a downy mildew fungus. *The Plant Cell* **2**, 437–445.
- Lam S.K., Siu C.L., Hillmer S., Jang S., An G., Robinson D.G. & Jiang L. (2007) Rice SCAMP1 defines clathrin-coated, trans-Golgi-located tubular-vesicular structures as an early endosome in tobacco BY-2 cells. *The Plant Cell* **19**, 296–319.
- Landschulz W.H., Johnson P.F. & McKnight S.L. (1988) The leucine zipper: a hypothetical structure common to a new class of DNA binding proteins. *Science* **240**, 1759–1764.
- Li J., Brader G., Kariola T. & Palva E.T. (2006) WRKY70 modulates the selection of signaling pathways in plant defense. *The Plant Journal* **46**, 477–491.
- Livak K.J. & Schmittgen D.T. (2001) Analysis of relative gene expression data using real-time quantitative PCR and the $2^{-\Delta\Delta CT}$ method. *Methods* **25**, 402–408.
- Mayo K.J., Gonzales B.J. & Mason H.S. (2006) Genetic transformation of tobacco NT1 cells with *Agrobacterium tumefaciens*. *Nature Protocol* **1**, 1105–1111.
- Miao Y. & Jiang L. (2007) Transient expression of fluorescent fusion proteins in protoplasts of suspension cultured cells. *Nature Protocol* **2**, 2348–2353.
- Nadimpalli R., Yalpani N., Johal G.S. & Simmons C.R. (2000) Prohibitins, stomatins, and plant disease response genes compose a protein superfamily that controls cell proliferation, ion channel regulation, and death. *Journal of Biological Chemistry* **275**, 29579–29586.
- Nebenführ A., Ritzenthaler C. & Robinson D.G. (2002) Brefeldin A: deciphering an enigmatic inhibitor of secretion. *Plant Physiology* **130**, 1102–1108.
- Nürnberg T., Brunner F., Kemmerling B. & Piater L. (2004) Innate immunity in plants and animals: striking similarities and obvious differences. *Immunological Reviews* **198**, 249–266.
- Remans T., Smeets K., Opendakker K., Mathijssen D., Vangronsveld J. & Cuypers A. (2008) Normalisation of real-time RT-PCR gene expression measurements in *Arabidopsis thaliana* exposed to increased metal concentrations. *Planta* **227**, 1343–1349.
- Robatzek S., Chinchilla D. & Boller T. (2006) Ligand-induced endocytosis of the pattern recognition receptor FLS2 in *Arabidopsis*. *Genes & Development* **20**, 537–542.
- Rooke L., Byrne D. & Salgueiro S. (2000) Marker gene expression driven by the maize ubiquitin promoter in transgenic wheat. *Annals of Applied Biology* **136**, 167–172.
- Rostoks N., Schmierer D., Kudrna D. & Kleinhofs A. (2003) Barley putative hypersensitive induced reaction genes: genetic mapping, sequence analyses and differential expression in disease lesion mimic mutants. *Theoretical and Applied Genetics* **107**, 1094–1101.
- Russinova E., Borst J.W., Kwaaitaal M., Caño-Delgado A., Yin Y., Chory J. & de Vries S.C. (2004) Heterodimerization and endocytosis of *Arabidopsis* brassinosteroid receptors BRI1 and AtSERK3 (BAK1). *The Plant Cell* **16**, 3216–3229.
- Saitou N. & Nei M. (1987) The neighbor-joining method: a new method for reconstructing phylogenetic trees. *Molecular Biology and Evolution* **4**, 406–425.
- Sambrook J. & Russel D.W. (2001) *Molecular Cloning: A Laboratory Manual*. Cold Spring Harbor Laboratory Press, New York, NY, USA.
- Schenk P.M., Kazan K., Manners J.M., Anderson J.P., Simpson R.S., Wilson I.W., Somerville S.C. & Maclean D.J. (2003) Systemic gene expression in *Arabidopsis* during an incompatible interaction with *Alternaria brassicicola*. *Plant Physiology* **132**, 999–1010.
- Shah K., Russinova E., Gadella T.W. Jr, Willemse J. & De Vries S.C. (2002) The *Arabidopsis* kinase-associated protein phosphatase controls internalization of the somatic embryogenesis receptor kinase 1. *Genes & Development* **16**, 1707–1720.
- Shanmugam V. (2005) Role of extracytoplasmic leucine rich repeat proteins in plant defence mechanisms. *Microbiological Research* **160**, 83–94.
- Song W.Y., Wang G.L., Chen L.L., et al. (1995) A receptor kinase-like protein encoded by the rice disease resistance gene, *Xa21*. *Science* **270**, 1804–1806.
- Spoel S.H., Johnson J.S. & Dong X. (2007) Regulation of tradeoffs between plant defenses against pathogens with different lifestyles. *Proceedings of the National Academy of Sciences of the United States of America* **104**, 18842–18847.
- Sun X., Cao Y., Yang Z., Xu C., Li X., Wang S. & Zhang Q. (2004) *Xa26*, a gene conferring resistance to *Xanthomonas oryzae* pv. *oryzae* in rice, encodes an LRR receptor kinase-like protein. *The Plant Journal* **37**, 517–527.
- Tamura K., Dudley J., Nei M. & Kumar S. (2007) MEGA4: Molecular Evolutionary Genetics Analysis (MEGA) software version 4.0. *Molecular Biology and Evolution* **24**, 1596–1599.
- Tornero P., Mayda E., Gómez M.D., Cañas L., Conejero V. & Vera P. (1996) Characterization of LRP, a leucine-rich repeat (LRR) protein from tomato plants that is processed during pathogenesis. *The Plant Journal* **10**, 315–330.

- Tse Y.C., Mo B., Hillme S., Zhao M., Lo S.W., Robinson D.G. & Jiang L. (2004) Identification of multivesicular bodies as pre-vacuolar compartments in *Nicotiana tabacum* BY-2 cells. *The Plant Cell* **16**, 672–693.
- Uknes S., Mauch-Mani B., Moyer M., Potter S., Williams S., Dincher S., Chandler D., Slusarenko A., Ward E. & Ryals J. (1992) Acquired resistance in *Arabidopsis*. *The Plant Cell* **4**, 645–656.
- Wang Z.Y., Seto H., Fujioka S., Yoshida S. & Chory J. (2001) BRI1 is a critical component of a plasma-membrane receptor for plant steroids. *Nature* **410**, 380–383.
- Weigel D. & Glazebrook J. (2006) Transformation of *Agrobacterium* using the freeze-thaw method. *Cold Spring Harbor Protocols* doi: 10.1101/pdb.prot4666.
- Xiao F., Tang X. & Zhou J.M. (2001) Expression of 35S::Pto globally activates defense-related genes in tomato plants. *Plant Physiology* **126**, 1637–1645.
- Yoo S.D., Cho Y.H. & Sheen J. (2007) *Arabidopsis* mesophyll protoplasts: a versatile cell system for transient gene expression analysis. *Nature Protocol* **2**, 1565–1572.
- Yoshimura S., Yamanouchi U., Katayose Y., Toki S., Wang Z.X., Kono I., Kurata N., Yano M., Iwata N. & Sasaki T. (1998) Expression of *Xal*, a bacterial blight-resistance gene in rice, is induced by bacterial inoculation. *Proceedings of the National Academy of Sciences of the United States of America* **95**, 1663–1668.
- Zhang Q., Shi A.N., Yang W.C. & Wang C.L. (1996) Breeding of three near-isogenic japonica rice lines with different major genes for resistance to bacterial blight. *Acta Agronomica Sinica* **22**, 135–141.
- Zipfel C., Kunze G., Chinchilla D., Caniard A., Jones J.D., Boller T. & Felix G. (2006) Perception of the bacterial PAMP EF-Tu by the receptor EFR restricts *Agrobacterium*-mediated transformation. *Cell* **125**, 749–760.

Received 12 May 2009; received in revised form 6 July 2009; accepted for publication 16 August 2009

SUPPORTING INFORMATION

Additional Supporting Information may be found in the online version of this article:

Figure S1. Negative control of immunogold electron microscopy. Immunogold electron microscopy was performed by just adding the gold labelled secondary antibodies. (a) Without the primary OsLRR1 antibodies, no gold particles could be observed on plasma membrane, cell wall and other organelles. (b) Comparison between unlabelled and OsLRR1-labelled clathrin-coated vesicles. The left image magnified from (a) displayed no signals of gold particles. The middle and right images from Fig. 4b of the main manuscript showed the signals of gold particles representing OsLRR1 localization. Bars = 100 nm.

Figure S2. Western blot of OsLRR1 using culture medium. Concentrated culture media were obtained from rice suspension cells (a) or transgenic tobacco BY-2 cells expressing the OsLRR1-GFP fusion protein (b, c). Total proteins from cells were used as the positive control. The detection was performed using OsLRR1 antibodies (a, b) or GFP antibodies (c). No OsLRR1 protein or OsLRR1-GFP fusion protein signals could be detected in the media. Ten

micrograms of protein was loaded onto each lane. Silver staining of the protein gels was shown to illustrate protein loading.

Figure S3. The effects of the flg22 application and bacteria incubation on the subcellular localization of OsLRR1. Transgenic tobacco BY-2 cells expressing the OsLRR1-GFP fusion protein were subjected to no treatment (a) or application of flg22 (b), *E. coli* (c), and *Pst. DC3000* (d). The subcellular localization of OsLRR1-GFP remained unchanged under all conditions tested. Bars = 20 μ m

Figure S4. Sequence alignment and hydrophobicity analysis of HIR1 homologs. (a) The amino acid sequences of CaHIR1, AtHIR1 and OsHIR1 were aligned to show their strong homology in primary sequence. Alignment was done using the ClustalW2 program (<http://www.ebi.ac.uk/Tools/clustalw2/index.html>). The red and blue boxes indicated the putative N-myristoylation site predicted by ScanProsite (<http://www.expasy.org/tools/scanprosite/>) and the position of the predicted transmembrane domains, respectively. (b) Hydrophobicity plots were performed with TopPred (<http://mobyle.pasteur.fr/cgi-bin/portal.py?form=toppred>) to predict transmembrane domains.

Figure S5. Lactophenol-trypan blue staining of leaves from wild type Col-0 and transgenic Col-0 expressing OsLRR1. Trypan blue staining was performed to detect dead cells on leaf tissues. Spontaneous micro-lesions were only found in the transgenic lines expressing OsLRR1 (right panel; indicated by arrows) but not in the untransformed control (left panel). Bars = 100 μ m

Figure S6. Expression of *OsLRR1* and rice *PR* genes in rice lines. Expression of *OsLRR1*, and the *PR* genes *OsPR1* and *OsPBZ1* were determined by real-time PCR as described in Fig. 8, using total leaf RNA from untransformed (WT) or OsLRR1 overexpressing transgenic rice lines. H7531, H7230 and H7232 are three independent transgenic lines. Relative gene expression levels were compared to WT (expression level set to 1). Error bars: standard deviation ($N = 3$).

Figure S7. Phenotypes of rice lines after inoculation with *Xoo*. Five-week-old seedlings of an OsLRR1 transgenic line and the untransformed parent (SN1033) were inoculated with *Xanthomonas oryzae* pv *oryzae* (*Xoo*) race LN44. The inoculation test was performed as described previously (Cheung *et al.* 2007).

Table S1. Primers for cloning and real-time PCR^a.

Video S1. Dynamic trafficking of OsLRR1-GFP. This movie is a time-lapse confocal analysis showing the dynamic trafficking of the punctated distribution pattern of OsLRR1-GFP in transgenic BY-2. The cytoplasmic organelles labelled by the OsLRR1-GFP fusion were not static, but highly mobile within the cell. The left panel showed the original OsLRR1-GFP fluorescent signals and the right panel was merged with DIC images. The time lapse covered a period of about 20 min with 60 frames.

Video S2. Co-localization of OsLRR1-GFP with FM4-64. This movie is a time-lapse confocal analysis showing the dynamic trafficking of the co-localized signals of OsLRR1-GFP and the endosomal pathway marker FM4-64, indicated as yellow-coloured dots in the cytosol. The

cytoplasmic organelles labelled by co-localized signals were not static, but highly mobile within the cell. The left panel showed the OsLRR1-GFP fluorescent signals and the right panel was merged with the signals of FM4-64. The time lapse covers a period of about 9 min with 40 frames.

Please note: Wiley-Blackwell are not responsible for the content or functionality of any supporting materials supplied by the authors. Any queries (other than missing material) should be directed to the corresponding author for the article.